Low Temperature Noise Measurement of an InAs/GaSb-based nBn MWIR Detector

Vincent M. Cowan[*1], *Christian P. Morath*[1], *Stephen Myers*[2], *Nutan Gautam*[2], *Sanjay Krishna*[2]
[1]Air Force Research Laboratory --Space Vehicles Directorate, 3550 Aberdeen Ave SE, Kirtland AFB, NM 87117, USA;
[2]Center for High Technology Materials, University of New Mexico, Albuquerque, NM 87106, USA

ABSTRACT

Recent experiments on conventional p-on-n and n-on-p Type II superlattices (SLS) infrared detectors still indicate larger than theoretically predicted dark current densities, despite the well known suppression of the Auger recombination mechanism. Rather, dark current in SLS is thought to still be limited by trap-assisted tunneling in the depletion region and surface leakage currents resulting from lack of fully passivated mesa sidewalls. An emerging infrared detector technology utilizing a unipolar, single-band barrier design, the so-called *nBn* architecture, potentially suppresses these remaining noise current mechanisms. In this report, measurements of the noise current spectral density of a mid-wave infrared nBn detector, composed of a type-II InAs/GaSb strain layer superlattice (SLS) absorber (*n*) and contact (*n*) layers with an AlGaSb barrier (*B*), under low-temperature, low-background conditions are presented. Here, noise was measured using a transimpedance amplifier incorporating a dewar-mounted feedback resistor R_F and source-follower MOSFET, both held at 77 K. This configuration confines high detector impedance issues to the dewar, minimizes Johnson noise due to the electronics, and enhances bandwidth by reducing stray capacitance. Features of the detector's noise spectrums at different bias are examined.

Keywords: nBn, SLS, InAs/GaSb, superlattice, noise, infrared

1. INTRODUCTION

1.1 Motivation

This paper presents recent experimental findings of low temperature noise measurements of an InAs/GaSb strained-layer superlattice (SLS) infrared (IR) detector utilizing a nBn design. The measurements were conducted such that the Trans-Impedance Amplifier (TIA) was cooled and located within close proximity to the detector under test. Thorough optical and electrical characterization as well as its performance as a function of total ionizing dose (TID) have been previously reported.[1, 2] Here, the characterizations results reported are focused on the nBn detectors noise spectra at varying applied voltages when held at 77 K. In exploring the utility of SLS based nBn detectors for imaging applications, it's paramount to gain an understand of the actual noise behavior of the detector under test, which is often substantially different than the dark current would indicate or masked by the external TIAs used in most conventional test beds.

1.2 Conventional Indirect Noise Measurement Technique for Single Element Detectors

In the detector community the importance of obtaining reliable yet timely performance results for single element detectors in growth-characterization campaigns is widely recognized. When performing a literature search of the methods used to measure noise of single element detectors it quickly becomes apparent that a common method of indirectly estimating the detector noise exists. In this method the detector noise is computed using the data collected from a conventional I-V measurement.[3,4] The expression for noise that has recently become more common in the literature is

* vincent.cowan@kirtland.af.mil

Infrared Technology and Applications XXXVII, edited by Bjørn F. Andresen, Gabor F. Fulop, Paul R. Norton,
Proc. of SPIE Vol. 8012, 801210 · © 2011 SPIE · CCC code: 0277-786X/11/$18 · doi: 10.1117/12.884808

Report Documentation Page

Form Approved
OMB No. 0704-0188

1. REPORT DATE	2. REPORT TYPE	3. DATES COVERED
2011		**00-00-2011 to 00-00-2011**

4. TITLE AND SUBTITLE	5a. CONTRACT NUMBER
Low Temperature Noise Measurement of an InAs/GaSb-based nBn MWIR Detector	5b. GRANT NUMBER
	5c. PROGRAM ELEMENT NUMBER
6. AUTHOR(S)	5d. PROJECT NUMBER
	5e. TASK NUMBER
	5f. WORK UNIT NUMBER
7. PERFORMING ORGANIZATION NAME(S) AND ADDRESS(ES) **Air Force Research Laboratory,Space Vehicles Directorate,3550 Aberdeen Ave SE,Kirtland AFB,NM,87117**	8. PERFORMING ORGANIZATION REPORT NUMBER
9. SPONSORING/MONITORING AGENCY NAME(S) AND ADDRESS(ES)	10. SPONSOR/MONITOR'S ACRONYM(S)
	11. SPONSOR/MONITOR'S REPORT NUMBER(S)

12. DISTRIBUTION/AVAILABILITY STATEMENT
Approved for public release; distribution unlimited

13. SUPPLEMENTARY NOTES

14. ABSTRACT

Recent experiments on conventional p-on-n and n-on-p Type II superlattices (SLS) infrared detectors still indicate larger than theoretically predicted dark current densities, despite the well known suppression of the Auger recombination mechanism. Rather, dark current in SLS is thought to still be limited by trap-assisted tunneling in the depletion region and surface leakage currents resulting from lack of fully passivated mesa sidewalls. An emerging infrared detector technology utilizing a unipolar, single-band barrier design, the so-called nBn architecture, potentially suppresses these remaining noise current mechanisms. In this report, measurements of the noise current spectral density of a mid-wave infrared nBn detector composed of a type-II InAs/GaSb strain layer superlattice (SLS) absorber (n) and contact (n) layers with an AlGaSb barrier (B), under low-temperature, low-background conditions are presented. Here, noise was measured using a transimpedance amplifier incorporating a dewar-mounted feedback resistor RF and source-follower MOSFET, both held at 77 K. This configuration confines high detector impedance issues to the dewar, minimizes Johnson noise due to the electronics, and enhances bandwidth by reducing stray capacitance. Features of the detector?s noise spectrums at different bias are examined.

15. SUBJECT TERMS

16. SECURITY CLASSIFICATION OF:			17. LIMITATION OF ABSTRACT	18. NUMBER OF PAGES	19a. NAME OF RESPONSIBLE PERSON
a. REPORT **unclassified**	b. ABSTRACT **unclassified**	c. THIS PAGE **unclassified**	**Same as Report (SAR)**	**8**	

$$j_N = \sqrt{2qJ + (4k_BT)/R_dA_d}, \quad (1)$$

where q is the electronic charge, J is the current density, k_B is Boltzman's constant, T is temperature, R_d is the dynamic resistance, and A_d is the diode area. Given that the noise j_N expressed here is in units of A/Hz$^{1/2}$ cm, equation (1) is convenient for estimating detectivity $D^* = R_{Peak} / j_N$, where R_{Peak} is the peak responsivity. However, this expression also assumes thermal noise and shot-noise with a photodiode-like unity gain G are the only noise sources, an assumption which may not necessarily always be valid. For example, evidence that barrier-style detectors may have $G > 1$ was observed in Ref. 5.[5]

The other significant issue with this noise expression is that it obviously does not account for $1/f$ noise or other potential noise sources, which may manifest in the signal-to-noise ratio at lower light levels. Focal plane arrays often run at frequencies ranging between 10-1000 Hz, making $1/f$ noise a distinct possibility.[6] So while a cursory inspection of detectors is possible using standard dark current measurements to estimate noise, it is nonetheless vital to understand how noise varies as a function of frequency to ultimately determine the minimum resolvable signal of the detector and thus its overall performance.

The simplest alternative, method to measure noise, rather than estimating it via dark current measurements, would be to use a commercially built TIA external to the dewar in conjunction with a standard dynamic signal or network analyzer. The difficulty encountered with this approach is that the noise generated by the combination of the amplifier, dewar, cabling and analyzer, is often much greater than that of the detector under test itself, the so-called *system*- or *amplifier*-limited scenario. The high noise floor can usually be attributed to a combination of thermal noise, electromagnetic interference (EMI), ground-loops, etc. Reducing each of these is key to measuring the detector noise. For example, the thermal noise current of the amplifier's feedback resistor i_j is given by

$$i_j = \sqrt{4k_BT\Delta f/R_f}, \quad (2)$$

where k_B is Boltzmann's constant, T is absolute temperature, Δf is bandwidth, and R_f is the feedback resistance. The only variables in equation (2) are T and R_f. The feedback resistance is determined by balancing considerations of noise and dynamic range; a larger R_f. reduces i_j, while a smaller R_f increases the amplifier's dynamic range and bandwidth ($\tau \sim C_fR_f$). Thus, a larger R_f is typically more ideal for noise measurements. The second variable T can only be reduced by cooling the feedback resistor. Cooling R_f from 300 K down to 77 K reduces i_j by the fraction $\sqrt{77/300} \sim 0.5$, which may be necessary if the detector noise is particularly small. Reducing other potential noise sources (i.e. EMI, ground-loops, etc.) requires a combination of proper shielding and grounding techniques.

The scope of this report is to present noise measurement results for a type-2 SLS nBn detector using both methods described above, as well as a different amplifier-technique that attempts to eliminate the system noise as much as possible. Here, the amplifier circuit includes a cooled input-MOSFET and feedback resistor, both located within close proximity to detector under test inside the cryogenic dewar. The results in the following compare the differences between each method and explore the change in noise with increasing detector current.

1.3 Detector Architecture

The nBn IR detector under test, illustrated in Figure 1, is composed of an InAs/GaSb SLS absorber (*n*) and contacts (*n*) with an $Al_xGa_{1-x}Sb$ barrier (*B*) grown by solid source molecular beam epitaxy (MBE). This particular detector architecture was developed and grown by the Center for High Technology Materials (CHTM) at the University of New Mexico. Solid source molecular beam epitaxy in a VG-80 system was used for growth. Specific details on the growth methods have been previously reported. Once grown, the material was processed using dry etching techniques and conventional optical photolithography. This resulted in the formation of both deep and shallow etch detector mesas shown in Figure 1 having dimensions of 410µm by 410µm with a 200µm circular window. The nBn detector did not receive an antireflection coating. Both the common back plane and the top contacts of the individual detectors were wire-bonded to a 68 pin leadless chip carrier (LCC).

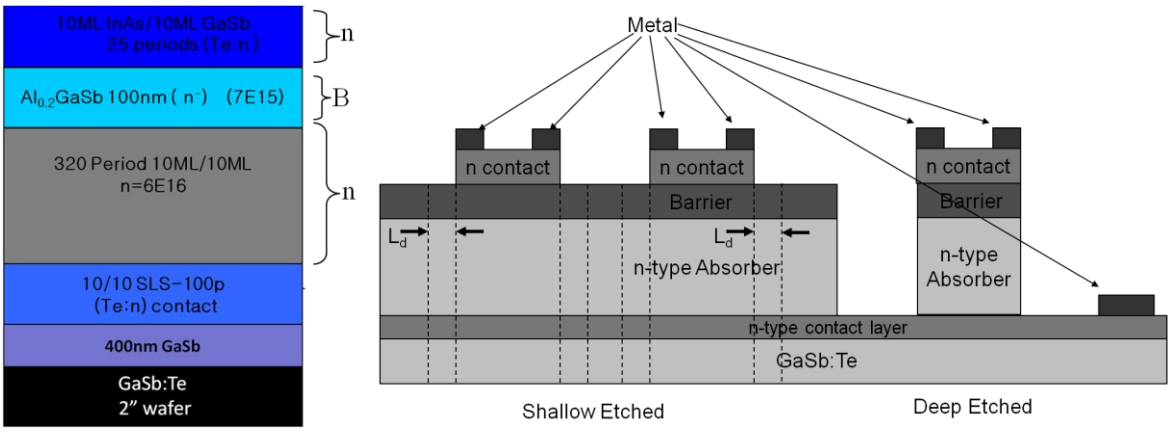

Figure 1. Schematic of the nBn wafer structure (left), shallow and deep etch profiles (right)

The orientation for positive bias used here is for the bias to be applied to the common back plane, while the tops of each individual detector were grounded. For this experiment the noise of both a shallow and deep-etched detector were measured. The detectors were consisted of a 410 x 410μm mesas with a 200μm diameter window etched through the top contact.

2. METHODOLOGY

2.1 Test Bed Overview

Figure 2 below shows a block diagram representation of the test bed used to acquire data presented in this paper. A TIA that includes a source-follower MOSFET input-stage and feedback resistor mounted inside the dewar was used to convert the detector noise current to an output voltage. The TIA was battery-powered for low noise. The noise spectrums from 1-10 kHz of the nBn detector under test were measured using a Stanford Research Systems model SR770 FFT network analyzer using the output of the TIA. The analyzer was read-out and controlled remotely via computer. A detector bias was applied using a Stanford Research Systems model SR570 low noise pre-amplifier.

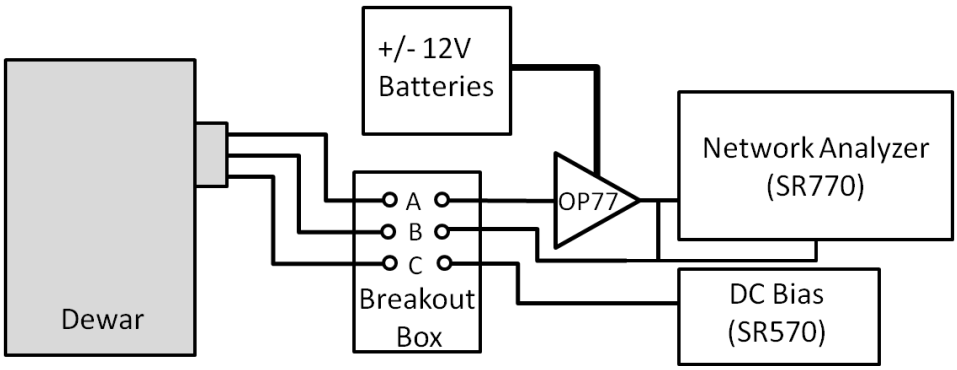

Figure 2. Block diagram representation of noise measurement apparatus. The letters A, B, and C are cross-referenced in Fig. 3.

2.2 Trans-Impedance Amplifier Circuit

The TIA circuit used to characterize the nBn detector is shown in Figure 3. This circuit is fundamentally the same as that used by others performing noise measurements in this fashion with exception of the size of the feedback resistor.[7,8] The MOSFET-based input-stage is a source-follower circuit, which serves to help match the high impedance of the detector to

the low input impedance of the OP77 op-amp that is external to the dewar and to provide significant current gain to drive the dewar cabling connected to the op-amp's inverting input.

This method of noise measurements affords several advantages. First, the virtual ground of the I-TIA is now within the dewar itself and closer to the detector and feedback resistor. The conventional long lead which traditionally brings a small current to the TIA's inverting input (required for traditional TIA configurations) and is prone to EMI is effectively eliminated here. Additionally, the thermal noise discussed in equation (1) can be reduced significantly by cooling the feedback resistor and MOSFET, which are both anchored to the liquid nitrogen bath. Furthermore, stray RC coupling can be minimized resulting in a reduction of the current leakage in cabling. The available current paths are reduced to just those shunting the detector under test. The commensurate reduction in input capacitance also reduces the "boosting" effect to amplifier voltage noise.

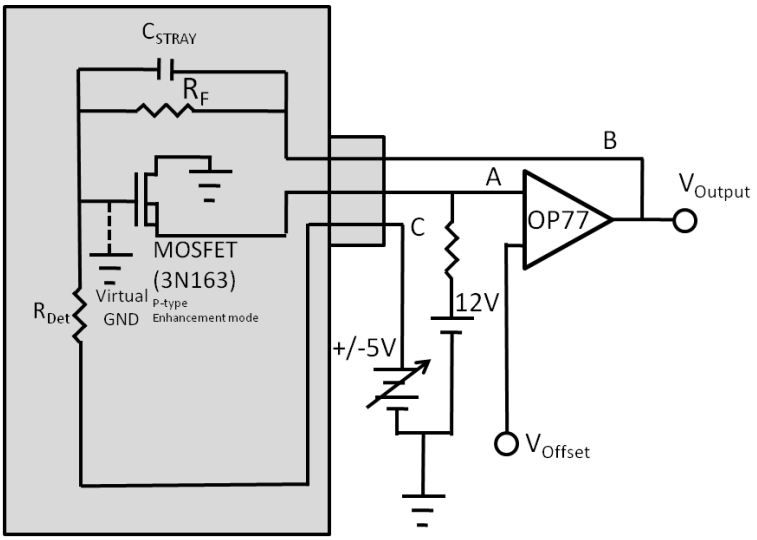

Figure 3. Dewar mounted Trans-Impedance Amplifier circuit layout

In this TIA circuit a bias is applied across one end of the detector under test and earth ground. However, the current measured through the detector is in reference to a virtual ground that is isolated from earth ground. With this circuit layout only the current flowing through the detector under test and therefore due to the summing point constraint through the feedback resistor, R_F is measured.

3. RESULTS & DISCUSSION

3.1 Baseline tested noise measurements

The baseline noise of the measurement setup is shown by the black trace in Figure 4 below. This is the noise spectrum measured while the opposite end of the detector is left open (disconnecting the bias source), which eliminates the detector as a noise source and eliminates the current through R_F as a potential noise source. This was also the configuration that was used to set the V_{Offset}, such that V_{Output} = 0 V, which we refer to herein as "balancing the circuit." In this case, the noise includes the thermal noise of R_F, the MOSFET and the op-amp.

When the detector is under bias there will be additional noise sources present. In addition to the actual noise present from the sample under test there are several other noise sources associated with the measurement setup that needed to be measured to establish the baseline noise. These additional noise sources include the following; noise in fluctuations in the gate voltage of the MOSFET, op-amp noise, noise caused from current flowing through the feedback resistor. The combined noise from all of the noise sources mentioned results in the baseline noise spectrum shown in Figure 4.

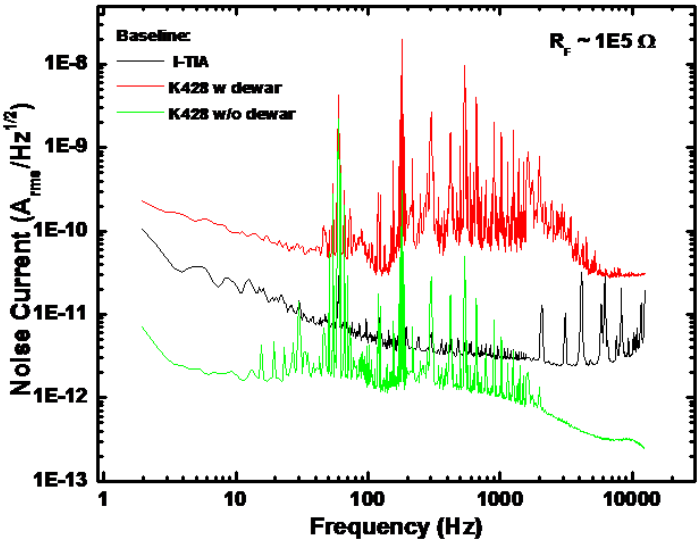

Figure 4. Baseline noise current spectra from internal and external TIAs

The other two plots, shown for comparison purposes, are of the minimum noise floor spectrums of a conventional external Kiethley model 428 TIA, when both connected to the dewar (red trace) and completely disconnected (green trace). The gain setting on the external TIA for these plots was 10^5 V/A, similar to the $R_F \sim 10^5$ Ω of the internal TIA. The green trace is very close to the manufacturer's expectation for the amplifier noise current. Comparing the green and red traces, it appears that simply attaching the external TIA to the dewar itself leads to a dramatic increase in the noise floor of roughly 2-orders of magnitude and additional EMI. The black trace illustrates the advantage of using the internal-TIA setup. Here, both the noise floor and the EMI, indicated by the spikes at 60 Hz and its higher harmonics, are vastly reduced. The measured output noise for the I-TIA (black trace) most likely reflects the 1/f noise of the source-follower MOSFET. The noise amplitude, however, was above the expected level based on previous work, which may reflect the difference in the feedback resistor or be related to the MOSFET.[8]

3.2 Forward bias noise current spectra

Noise current spectrum were taken for both the shallow and deep etch nBn detectors as a function of forward bias and are shown in Figure 5. In both cases, the noise spectrum rapidly increases with bias at low frequencies, while somewhat less so at higher frequencies. The noise spectrum of the shallow etched device when forward biased showed a slightly greater dependence on applied bias initially than the deep etched detector; however, by V_B = .2 V they are both very close to one another. Over this bias range the noise current's of both detectors changed by roughly 1.5 orders of magnitude.

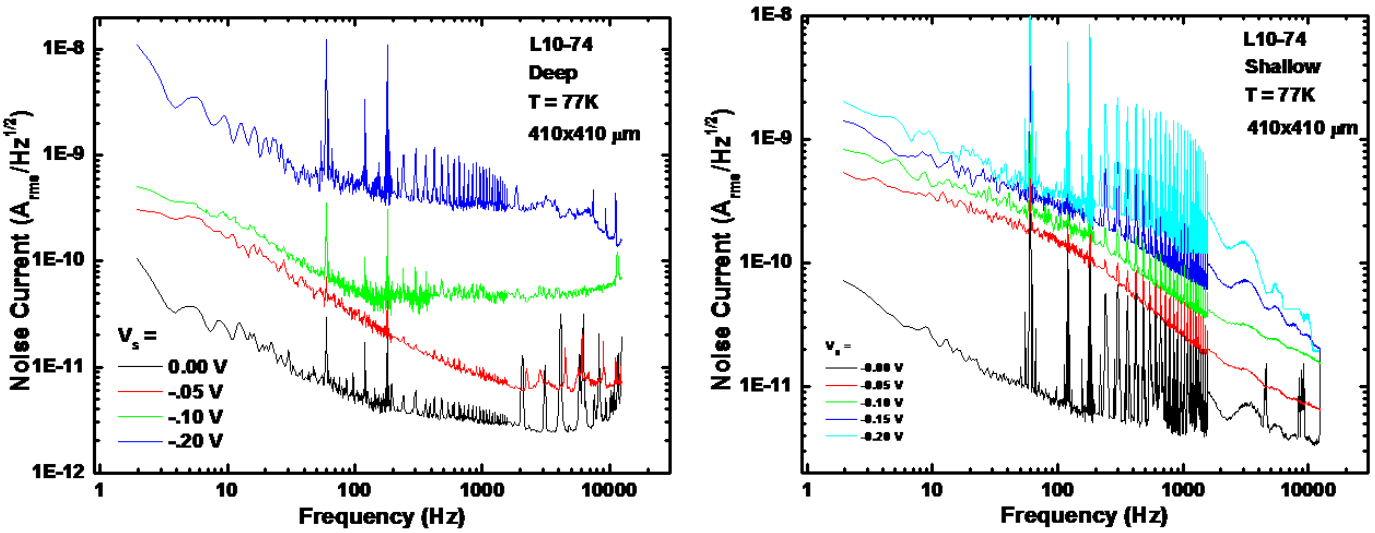

Figure 5. Noise current spectrum as a function of forward bias for deep (left), and shallow (right) etch devices

3.3 Reverse bias noise current spectra

Noise current spectrums were also taken for both the shallow and deep etch nBn detectors as a function of reverse bias and are shown in Figure 5. Here, the increase is much slower that what was observed in Figure 6, with a roughly similar noise magnitude increase observed for a bias up to V_B = .5 V. Also, in the reverse bias it appears the noise increases more rapidly for the shallow etch detector compared with the deep etched.

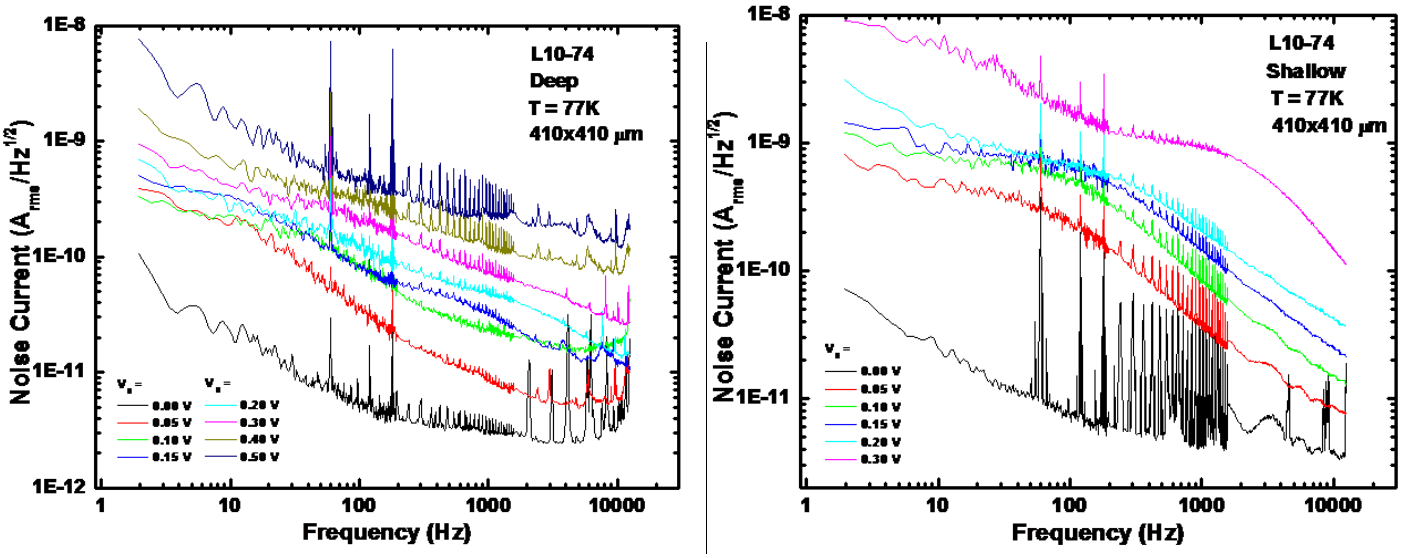

Figure 6. Noise current spectrum as a function of reverse bias for deep (left), and shallow (right) etch devices

3.4 Comparison of noise current as a function of applied bias and frequency

From the data in Figures 5 and 6, plots of the noise current at specific frequencies versus bias voltage, shown in Figure 7, were derived. Here, for comparison purposes, the noise current computed using equation (1) is also shown (solid line, black trace). Comparing this trace with the others, the noise estimate based on the dark current is roughly 1.5 orders smaller than the lowest noise measurements at 1 kHz and 10 kHz. The noise floor of the internal TIA at 10 kHz and the calculated thermal noise of R_F are also shown (dotted black lines). This comparison suggests estimating the noise based on the dark current may not always be valid as it presumes to know exactly what noise sources exist, typically ignoring the *1/f* noise source which is difficult to model. The second thing to note from the plots in Figure 6 is that the shapes of the noise current versus bias plots are roughly similar to the noise estimate plot. This suggests that there may be some connection between dark current and noise, although not the one explicitly expressed in equation (1).

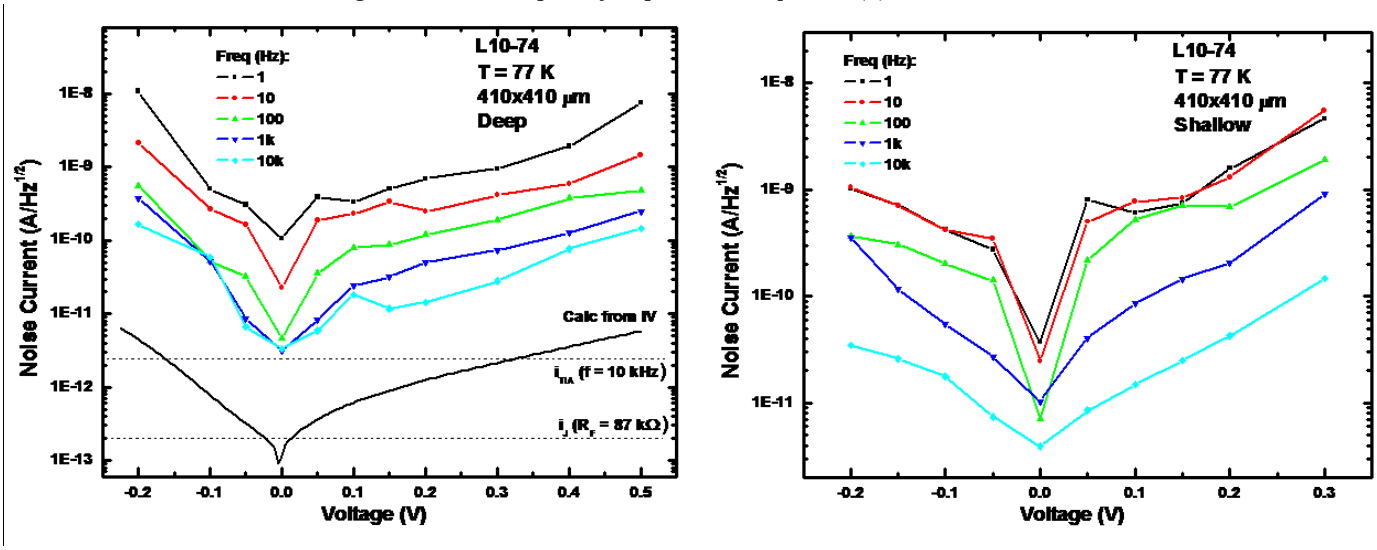

Figure 7. Noise currents as a function of bias and frequency deep (left), and shallow (right) etch devices

3.5 Noise current as a function of current

To further ascertain the nature of the noise present in nBn detectors, the dependence of the noise currents on the square root of the current was investigated. This dependence is expected based on the Shot noise formula for current flowing through a junction given by equation (3) in the following.

$$I_N = (2qI\Delta F)^{1/2}, \tag{3}$$

where q is the electronic charge, I is the current and ΔF is the bandwidth. The results of this analysis are shown in Figure 8 below. These plots show that a linear relationship between noise and current exists at 1 kHz and 10 kHz for certain current ranges. Fitting a line to these linear regions the slopes of each were determined; the slopes are listed on the plots in Figure 8. These slopes are all in the range of ~10^{-8} $C^{1/2}$, which is 2 orders of magnitude than the slope predicted by equation (3), equal to $(2q)^{1/2}$ ~ 5.7 x 10^{-10} $C^{1/2}$. This fact again suggests the measured noise is not related to shot-noise, despite the apparently linear relationship visible in Figure 8. The linear relationship between I_N and $I^{1/2}$, however, also precludes the noise from being directly attributable to *1/f*-noise, which typically has a linear dependence on current.

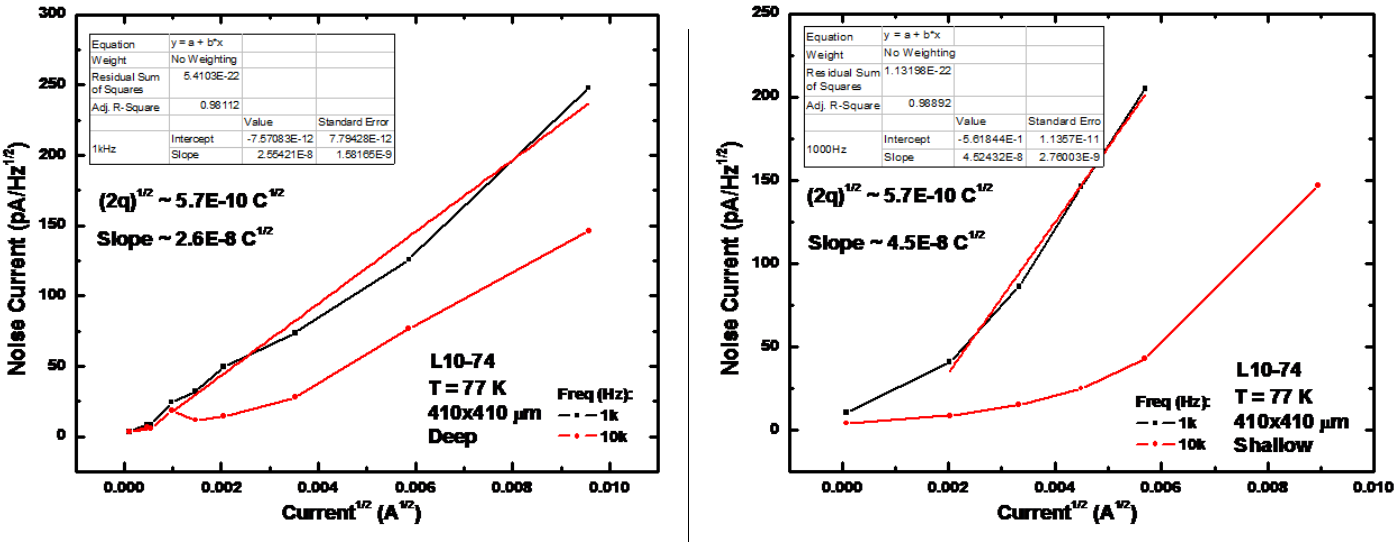

Figure 8. Further illustration of 1/f noise in deep (left), and shallow (right) etched nBn detectors

4. CONCLUSION

A measurement setup was constructed utilizing a cooled MOSFET and feedback resistor to measure noise spectrums of a infrared nBn detector, composed of a type-II InAs/GaSb strain layer superlattice (SLS) absorber (*n*) and contact (*n*) layers with an AlGaSb barrier (*B*). Discrepancies between noise currents reporting methods in literature and this work were presented. A comparison of the noise versus bias voltage and square root of device current was done. The nBn detector was shown to have some aspects of *1/f*-noise, while at the same time showing a nearly linear relationship with $I^{1/2}$ for certain current ranges The latter is not typical of *1/f*-noise, which is normally linearly dependent on *I*. Similar noise performance was observed for both the deep and shallow etched devices

5. ACKNOWLEDGEMENTS

The authors would like to acknowledge Dr John Hubbs and his team from Infrared Radiation Effects Laboratory for their guidance. Likewise work was possible with the funding awarded under AFOSR Contract No. FA9550-09-1-0231 and AFRL Contract No. FA9453-07-C-0171.

REFERENCES

[1] V. M. Cowan, C. P. Morath, S. M. Swift, P. D. LeVan, S. Myers, E. Plis, and S. Krishna, "Electrical and Optical Characterization of InAs/GaSb-based nBn IR Detector," Proc. SPIE, Vol. 7780, 778006 (2010).

[2] V. M. Cowan, C. P. Morath, S. Myers, N. Gautam, and S. Krishna, "Electrical and Optical Characterization of InAs/GaSb-based nBn IR Detector," Proc. SPIE, Vol. 7945, 79451S (2011).

[3] E. Plis, S. Annamalai, K. T. Posani, S. Krishna, R. A. Rupani, and S. Ghosh, J. Appl. Phys. **100**, 014510 (2006).

[4] B.-M. Nguyen, S. Bogdanov, S. Abdollahi Pour, and M. Razeghi, Appl. Phys. Lett. **95**, 183502 (2009).

[5] A. Soibel, D. Ting, C. Hill, M. Lee, J. Nguyen, S. Keo, J. Mumolo and S. Gunapala, Appl. Phys. Lett. **96**, 111102 (2010).

[6] M. Gramer, D. Maestas-Jepson, Personal Communication (2011).

[7] J. E. Hubbs, D. C. Arrington, M. E. Grammer, and G. A. Dole, Opt. Eng. (Bellingham) 39, 2660 (2000).

[8] B. J. Klemme, C. P. Morath and D. T. Le, "Low-temperature noise measurements on quantum well infrared photodetectors", Proc. SPIE 5111, 162 (2003).